Solar Energy Materials and Solar Cells 168 (2017) 45–50

Contents lists available at ScienceDirect

Solar Energy Materials and Solar Cells

journal homepage: www.elsevier.com/locate/solmat

Preparation and characterization of mixed caesium-tin mixed salt of Keggin-type phosphovanadomolybdate. Application to photocatalytic chromate reduction

L. Dermèche[a], C. Rabia[a], G. Rekhila[b,*], M. Trari[b]

[a] Laboratory of Chemistry of Natural Gas, Faculty of Chemistry (USTHB), BP 32, 16111 Algiers, Algeria
[b] Laboratory of Storage and Valorization of Renewable Energies, Faculty of Chemistry (USTHB), BP 32, 16111 Algiers, Algeria

ARTICLE INFO

Keywords:
$CsSnPMo_{11}VO_{40}$
Keggin-type
Photoelectrochemistry
Chromate
Visible light

ABSTRACT

In this study, we are interested by the caesium-tin mixed salt of 1-vanado-11-molybdophosphoric acid ($CsSnPMo_{11}VO_{40}$) with Cs/Sn ~ 1, micro and mesoporous material with a large specific surface area and a good thermal stability. Caesium atoms in $Cs_3HPMo_{11}VO_{40}$ are partially substituted by tin in order to facilitate the electron transfer in the redox processes. The synthesis and characterization by BET measurement, inductively coupled plasma (ICP), X-ray diffraction (XRD), ^{31}P NMR, thermal analysis (TGA and DTA), UV–Vis and Raman spectroscopies, infrared technique of the Keggin-type compound $CsSnPMo_{11}VO_{40}$ are reported. The forbidden band (1.72 eV) is due to the crystal field splitting of Mo^{6+}: *4d* orbital in octahedral site and the compound exhibits a chemical stability at neutral pH and semiconducting properties due to molybdenum mixed valences. The intensity-potential (J-E) characteristic shows a small hysteresis while the capacitance measurement (C^{-2} - E) of the junction $CsSnPMo_{11}VO_{40}$/electrolyte in Na_2SO_4 electrolyte exhibits a rectifying behavior with a Schottky type barrier; the positive slope is characteristic of *n* type conduction with a flat band potential of −0.30 V_{SCE}. The electrochemical impedance spectroscopy (EIS) shows two overlapped semicircles attributed to the bulk contribution ($R_b = 168\ \Omega\ cm^2$) and grains boundaries ($R_{gb} = 806\ \Omega\ cm^2$). The depletion angle (−16°) is ascribed to a constant phase element (CPE, 67 µF cm^{-2}). The photosensitivity in the visible light involves *d–d* transition and the energy diagram shows the feasibility of the material for the $HCrO_4^-$ reduction upon visible light (109 mW cm^{-2}). The disappearance rate is found to be 4 mmol mn^{-1} (mg catalyst)$^{-1}$ and the chromate reduction obeys to a first order kinetic with a half-life of 83 mn.

1. Introduction

The polyoxometalates have attracted a great interest not only for their architectures, but also for their properties that can be modified by changing their size, shape, charge and chemical composition [1–4]. Most polyoxometalates possess extensive and reversible redox chemistry, and some of them contain multiple unpaired *d*-electrons that are delocalized to various degrees in these nanoscale structures [5]. The polyoxometalates are generally resistant to both oxidative and thermal degradations, and are chemically stable in a wide pH range. These collective properties have applications in magnetism, electrochemistry, biochemistry and catalysis. The applications of polyoxometalates were also demonstrated in the rechargeable lithium ion batteries [6] and light driven photocatalysis [7].

The mixed addenda phosphovanadomolybdic acid $CsSnPMo_{11}VO_{40}$ possesses attractive properties such as reduction potential, solubility, acidity, polarity, which are of central importance in the fields of the energy supply [8] and environmental protection [9]. A band gap (E_g) of ~ 2 eV, a cathodic flat band potential (E_{fb}) and environmentally friendly characteristics are the required criteria for materials used in the solar energy conversion [10,11]. So, in this work, we report the synthesis, the physical properties and photoelectrochemical characterization of caesium-tin mixed salt of Keggin-type phosphovanadomolybdate $CsSnPMo_{11}VO_{40}$. The photo-electrochemistry throws light on the optical transitions and the nature of electronic bands, permitting the construction of the energy diagram of the liquid/solid junction, a preamble of the photocatalysis [12].

The fundamental concept of the photoelectrochemical application has been demonstrated in the open literature [13] and the conduction band originating from *4d* metal parentage possesses a high energy, giving the compound a strong reducing power [14]. As application, the material was successfully used for the chromate reduction under visible

---

* Corresponding author.
E-mail address: rekhilagharib@yahoo.fr (G. Rekhila).

http://dx.doi.org/10.1016/j.solmat.2017.04.003
Received 15 August 2016; Received in revised form 2 February 2017; Accepted 4 April 2017

Table 1
Chemical composition from ICP and surface area of $Cs_xSn_yPMo_{11}V$.

Formula	Chemical composition (wt%)				Stoichiometrie coefficients				Surface area (m^2/g)
	P	Mo	V	X	P	Mo	V	X	
$Cs_{2.06}Sn_{0.97}PMo_{11}V$	1.41	43.82	2.10	4.80	1.09	11	0.99	0.97	79.0

light. Indeed, hexavalent chromium is toxic and its reduction to less harmful forms, namely Cr^{3+} is of high importance for the human health. The redox potential of Cr(VI) is more anodic than the conduction band of $Cs_xSn_yPMo_{11}VO_{40}$; the difference measures the driving force and exceeds the optimal value of 0.4 V for an efficient separation of electron/hole (e^-/h^+) pairs, leading to chromate reduction upon illumination.

2. Experimental

2.1. Heteropolysalt synthesis

$Cs_xSn_yPMo_{11}VO_{40}$ heteropolysalt (noted $CsSnPMo_{11}V$) was precipitated from $H_4PMo_{11}VO_{40}$, heteropolyacid (noted $H_4PMo_{11}V$), according to the following equation:

$$PMo_{11}VO_{40}^{4-} + x\ Cs^{+} + y\ Sn^{2+} \Leftrightarrow Cs_xSn_yPMo_{11}VO_{40} \quad (1)$$

$H_4PMo_{11}VO_{40}$ was prepared by the Tsigdinos method [15]. To 5 mL of aqueous solution of $H_4PMo_{11}VO_{40}$, $13H_2O$ (8 g, 4 mmol), 5 mL of Cs $(CO_3)_2$ (1 M) and 5 mL of $SnCl_2{\cdot}H_2O$ (0.6 M) were added under stirring; a dark green precipitate appeared immediately. After 2 h of agitation, the precipitate was filtered off and dried at room temperature.

2.2. Heteropolysalt characterization

The chemical composition of the heteropolysalt was determined by inductively coupled plasma (ICP) with an Activa JobinYvon Spectrometer. The BET surface areas were measured at liquid nitrogen temperature using a Micrometrics ASAP 2020 V1; prior the adsorption / desorption measurement; the samples were degassed at 130 °C (5 °C/min) for 2 h. The specific surface areas were determined from the linear part of the BET equation. The combined thermal gravimetry /thermal differential analysis (TG/TDA) were performed with a SDT-2960 thermal analyzer to follow the course of the synthesis reaction; the experiment was carried out in air flow at a heating rate of 10 °C/min, using 25–70 mg of the sample.

The infrared spectra were recorded with a Bruker Vector 22 FT-IR spectrometer in the range (400–4000 cm^{-1}) with samples (~ 2%) prepared as KBr disks. The ^{31}P NMR spectrum was measured at room temperature with a Bruker Avance 400 spectrometer, H_3PO_4 (85%) was used as external reference. The UV–Visible diffuse reflectance spectra were recorded in the region (200–800 nm) with a Specord 200 Plus spectrophotometer equipped with an integration sphere using polytetrafluoroethylene (PTFE) as standard.

The electrochemical measurements were performed at room temperature in a standard cell. The working electrode was prepared by pressing the powder (~ 100 mg) in pure graphite rod inserted in a glass assembly with a cylindrical cavity (3 mm diameter and 4 mm depth). The current density must be uniform; so the electrode was positioned in front of Pt auxiliary electrode and all potentials were quoted with respect to a saturated calomel electrode (SCE); the supporting electrolyte (Na_2SO_4 0.5 M) was used because of its high electro conductivity. The current-potential (J-E) characteristics were plotted in an aerated solution using a PGZ301 potentiostat (Radiometer analytical). The variation of the interfacial capacitance was measured at a frequency of 10 kHz. The electrochemical impedance spectroscopy (EIS) was studied over the frequency range (20 mHz–100 kHz) by a low perturbation technique which allows the system to remain in a pseudo equilibrium state. All electrochemical tests were plotted after stabilization of the open circuit potential (OCP = 520 mV).

The powder dispersion of chromate solution was achieved by magnetic agitation (400 rpm) in a batch Pyrex reactor; a period 160 min was necessary to reach the dark equilibrium. Then, the solution was illuminated by a tungsten lamp (200 W); the aliquots were withdrawn at regular time intervals and subjected to a vigorous centrifugation (2000 rpm, 20 mn) to separate the solid particles. The chromate reduction was followed by UV–visible spectrophotometry (λ_{max} = 350 nm) using Shimadzu UV1800 spectrophotometer; the photo catalytic efficiency was calculated from the following relation:

$$R(\%) = \{(C_o - C) / C_o\} \times 100 \quad (2)$$

where C_o and C (mg/L) are the initial and equilibrium $HCrO_4^-$ concentrations respectively. The solutions were prepared from reagents of analytical grade quality and distilled water.

3. Results and discussion

3.1. POM characterizations

The chemical composition determined by ICP and the specific surface area of $Cs_xSn_yPMo_{11}V$, are given in Table 1. The analysis of the salt was adjusted by considering 12 addenda atoms, molybdenum and vanadium per Keggin unit. The results agree with the nominal stoichiometry for phosphorous, vanadium and molybdenum; the number of Sn, introduced as counter-cations, is close to unity (X/P ~ 1).

The XRD pattern (Fig. 1a) of $CsSnPMo_{11}V$ is similar to that of $Cs_3HPMo_{11}VO_{40}$; the compound crystallizes in a cubic symmetry (SG: $Pn\bar{3}m$) with a lattice constant of 11.756 Å. After thermal treatment at 400 °C under oxygen flow (Fig. 1b), the pattern shows the presence of the orthorhombic phase α-MoO_3 with characteristic peaks (2θ = 12.5 and 27.5°), indicating the beginning of the phase decomposition corroborated by thermal analysis. The TG / TDA plots of $CsSnPMo_{11}V$ (Fig. 2) shows a weight loss before 200 °C accounting for 14.7%, assigned to the loss of the crystallization water and supported by two endothermic peaks at 64 and 118 °C on the DTA curve. The exothermic decomposition peak at 428 °C agrees with the XRD analysis. $CsSnPMo_{11}V$, prepared by precipitation from aqueous solution containing $H_4PMo_{11}VO_{40}$, presents cluster composition, a high BET surface area and a Keggin type structure. $CsSnPMo_{11}V$ has a BET surface area of

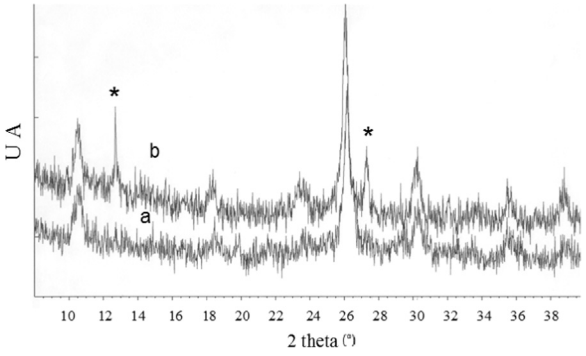

Fig. 1. XRD patterns of $CsSnPMo_{11}VO_{40}$, (a) Without pre-treatment. (b) After pretreatment at 400 °C under O_2 flow (4 h), (*) MoO_3.